CLICdp-Pub-2021-002
28 February 2021

Optimising top-quark threshold scan at CLIC using genetic algorithm

K. Nowak, A. F. Żarnecki

Faculty of Physics, University of Warsaw, Poland

Abstract

One of the important goals at the future e^+e^- colliders is to measure the top-quark mass and width in a scan of the pair production threshold. However, the shape of the pair-production cross section at the threshold depends also on other model parameters, as the top Yukawa coupling, and the measurement is a subject to many systematic uncertainties. Presented in this work is the study of the top-quark mass determination from the threshold scan at CLIC. The most general approach is used with all relevant model parameters and selected systematic uncertainties included in the fit procedure. Expected constraints from other measurements are also taken into account. It is demonstrated that the top-quark mass can be extracted with precision of the order of 30 to 40 MeV, including considered systematic uncertainties, already for 100 fb^{-1} of data collected at the threshold. Additional improvement is possible, if the running scenario is optimised. With the optimisation procedure based on the genetic algorithm the statistical uncertainty of the mass measurement can be reduced by about 20–30%. Influence of the collider luminosity spectra on the expected precision of the measurement is also studied.

This work was carried out in the framework of the CLICdp Collaboration

1 Introduction

The Compact Linear Collider (CLIC) is a linear e^+e^- collider project, that is considered as a possible next large infrastructure at CERN [1, 2]. CLIC is proposed as a staged machine running at energies from 380 GeV up to 3 TeV. The physics program of the first CLIC energy stage, at 380 GeV, focuses on precise measurements of the Higgs boson properties including its couplings to other SM particles [3] and a study of top-quark production and decays, incorporating an energy scan over the $t\bar{t}$ production threshold [4].

Precise measurement of the top-quark mass is essential for the understanding of the Higgs mechanism, electroweak symmetry breaking and for constraining many "new physics" scenarios. Scanning the threshold for top-quark pair production, $e^+e^- \to t\bar{t}$, was proposed as the method for top-quark mass measurement even before the top quark was actually discovered [5–7]. As the production cross-section can be calculated with a high degree of precision using theoretically well-defined top mass definitions [8] it is currently assumed to be the most precise method for top-quark mass determination and least sensitive to theoretical uncertainties.

Scan scenario with ten energy points separated by 1 GeV, with 10 fb^{-1} of data collected at each energy is considered as a baseline scenario for CLIC, as shown in Fig. 1. Detailed study [4] showed that expected statistical uncertainty on the mass is around 21 MeV and on the top-quark width - 51 MeV. However, systematic uncertainties are expected to limit the ultimate precision. In particular, mass uncertainty originating from the uncertainty of the strong coupling is estimated to be about 30 MeV [9]. The combined theoretical, parametric and experimental systematic uncertainties are expected to be in the range 40 MeV to 70 MeV, depending on the assumptions [4].

While these results are very encouraging, they were obtained from the threshold scan fit taking only the two model parameters, top-quark mass and width, into account. Yet, threshold cross-section shape depends also on other parameters, as the top Yukawa coupling and the strong coupling constant. Fit results are also sensitive to the normalisation of the model predictions and the background level estimates. The main goal of the presented study was to quantify the influence of additional model parameters, and related uncertainties, on the precision of top-quark mass determination at CLIC. By including corresponding parameter variations in the fit, influence of the considered systematic uncertainties can also be reduced.

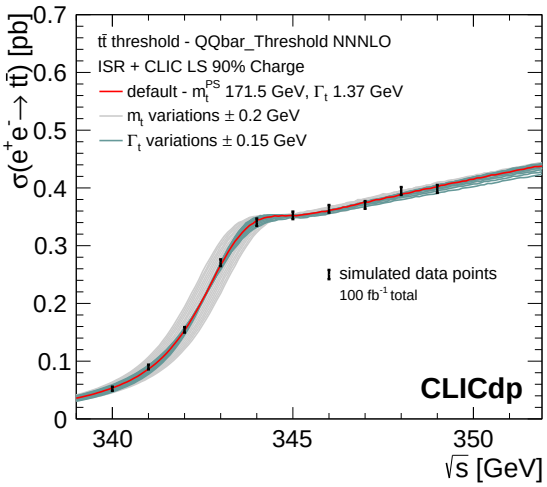

Figure 1: Illustration of a top-quark threshold scan at CLIC with a total integrated luminosity of 100 fb^{-1}. The bands around the central cross section curve show the dependence of the cross section on the top-quark mass and width, the error bars on the simulated data points show the expected statistical uncertainties of the cross section measurement. Figure taken from [4].

Parameter		Nominal	Min.	Max.	Step
top-quark mass	m_t	171.5 GeV	171.4 GeV	171.6 GeV	25 MeV
top-quark width	Γ_t	1.37 GeV	1.17 GeV	1.57 GeV	0.05 GeV
top Yukawa coupling	y_t	1.0	0.6	1.4	0.1
strong coupling constant	α_s	0.1185	0.1145	0.1225	0.001
overall renormalisation scale	μ	80 GeV			
nonresonant contr. scale	μ_w	350 GeV			
data normalisation	α	1			
background contribution	f_{bg}	73 fb	61 fb	85 fb	3 fb

Table 1: Parameters used as an input to `QQbar_threshold` (upper part of the table) and normalisation uncertainties considered in the analysis (lower part). Top-quark Yukawa coupling, y_t, is given relative to SM predictions. Overall renormalisation scale, μ, and the energy scale for nonresonant contributions, μ_w, were not varied in the described study. Range and step values are also not indicated for the overall data normalisation factor α, as it is evaluated analytically in the fit procedure (see Section 3.2 for details).

As the baseline running scenario seems to be conservative, the additional objective of the study was to investigate to what extent statistical uncertainties can be reduced when using the optimised running scenario. The scan optimisation is possible only if the top-quark mass is already known to $\mathcal{O}(100\,\text{MeV})$. If this level of precision is not reached by earlier measurements, an initial scan with fewer energy points can be required, with only a small fraction of total integrated luminosity dedicated to the threshold scan, see eg. [10]. However, suggesting any realistic running scenario, when the scan sequence is adjusted basing on the already collected scan data, is a much more complex problem and is beyond the scope of this work. Results included in this paper supersede results presented previously in [11–14].

2 Modelling of the threshold scan

In this chapter the procedure developed to model the top-quark pair production cross section measurements in a threshold scan at CLIC is described. Two elements are used to calculate the expected cross section values: theoretical predictions given in terms of the cross section templates and the expected luminosity spectra for CLIC.

2.1 Cross-section templates

Considered in the presented study are the cross section templates generated, assuming different values of top quark parameters, using `QQbar_threshold` software [15, 16]. Parameters used as an input to `QQbar_threshold` calculations are listed in the upper part of Tab. 1. Nominal cross section template was first generated for nominal values of all parameters. Three top-quark parameters considered in the study: mass, m_t, width, Γ_t, and Yukawa coupling relative to SM prediction, y_t, as well as the strong coupling constant, α_s, were then varied in small steps, corresponding to the expected experimental sensitivities, from their nominal values, resulting in additional cross section templates. Total of 274 templates were generated for different variations of model parameters. Each of those templates consists of 300 points representing cross-section for energy in range from 330 to 360 GeV. Examples of cross-section templates are shown in Fig. 2. Initial state radiation was included in the template cross section calculations.

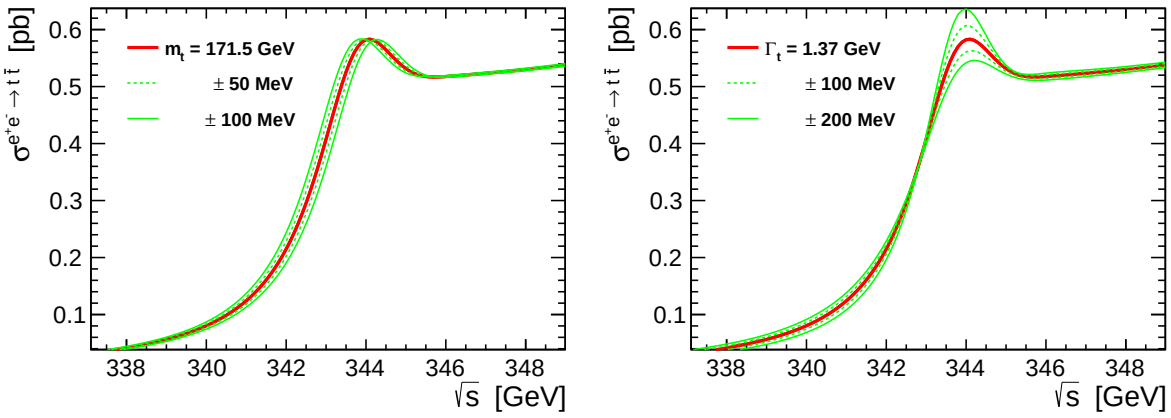

Figure 2: Examples of cross-section templates generated using `QQbar_threshold` software for different values of top-quark mass (left) and width (right) [17].

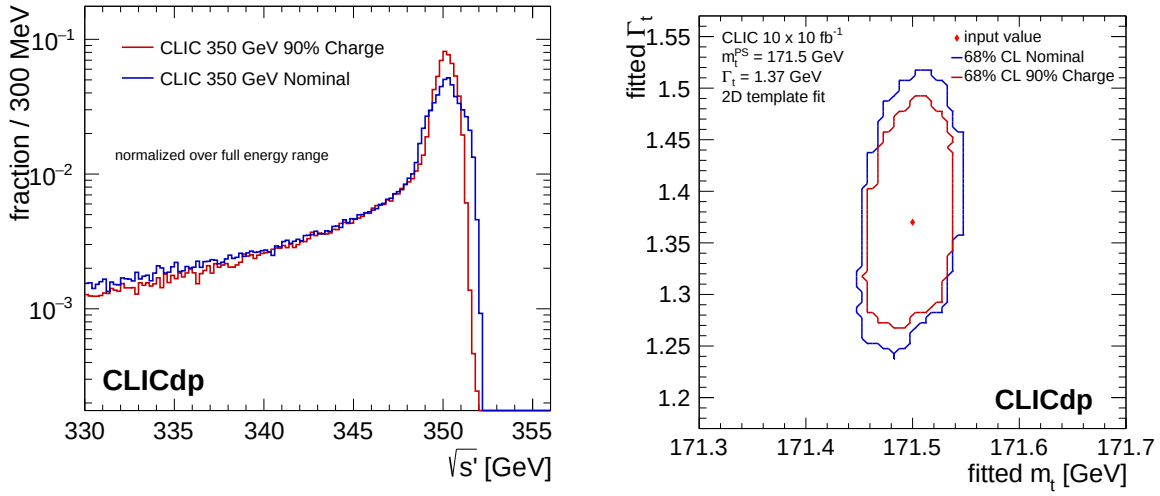

Figure 3: Left: two scenarios of the CLIC luminosity spectrum for a threshold scan, one based on the nominal accelerator parameters (Nominal) and one optimised for reduced beamstrahlung (90% charge). Right: 68% CL statistical uncertainty contours of the top-quark mass and width fits to the top threshold scan data, for two considered liminosity spectra scenarios, assuming an integrated luminosity of 100 fb^{-1} in both cases. Figures taken from [4].

2.2 Luminosity spectra

In order to take into account environment of the experiment, theoretical cross section templates, as generated with the `QQbar_threshold`, were convoluted with the expected CLIC luminosity spectra to obtain final cross-section templates used in the analysis. Two luminosity spectra were considered for the threshold scan: the nominal spectra expected for the first stage of CLIC, and the one with reduced bunch charge (90% charge), which allows to obtain narrower energy spectra at the cost of reduced instantaneous luminosity. Previous study [4] showed that the reduced charge option results in smaller statistical uncertainties of the threshold fit, see Fig. 3, and this spectra was therefore used for the presented study.

2.3 Reference scenario

At the first energy stage CLIC is assumed to run at the energy of 380 GeV, which was selected for optimising both the Higgs boson and top quark measurements. With 1 ab^{-1} of total integrated luminosity at this stage, a dedicated scan of 100 fb^{-1} is planned at the $t\bar{t}$ threshold. As already mentioned above, the baseline scenario of the threshold scan assumes running at 10 equidistant energy points taking 10 fb^{-1} of data for each value of $\sqrt{s}$. When generating simulated measurements (pseudo-data), the overall top-pair event reconstruction efficiency of 70.2% (including the relevant branching fractions) was assumed, and the background contribution remaining after the event selection procedure corresponding to the cross section of 73 fb [18]. Reconstruction efficiency is assumed to be independent of the collision energy (in the considered energy range) and of the model parameters.

2.4 Systematic uncertainties

In addition to the variations of the `QQbar_threshold` input parameters, as listed in the upper part of Tab. 1, possible variations of the overall data normalisation, α, and of the assumed background contribution, f_{bg}, were also considered in the modelling of the threshold scan results. Data normalisation factor α covers possible systematic variations due to the luminosity measurement, event selection efficiency or normalisation of the theoretical predictions. Uncertainties on the overall data normalisation, Δ, on the background normalisation, δ_{bg}, and on the value of the strong coupling constant, σ_α are considered as the sources of the systematic uncertainties in the extraction of the top-quark mass and other model parameters. If not stated otherwise, relative uncertainty of 1% is assumed for the overall data normalisation [1], while uncertainty of 2% is used for the background contribution. Strong coupling constant, α_s, is assumed to be known to 0.001.

3 Fit procedure

3.1 Simulated experiments

For each simulation of the threshold scan measurement, one of the cross section templates (convoluted with the luminosity spectra) is selected as the base for pseudo-experiment generation. By this choice, "true" values of top quark parameters are chosen for the considered fit scenario. Unless specified otherwise, nominal parameter values (and nominal template) were used in all calculations.

Selected template is used to generate a set of data corresponding to the expected scan results at CLIC, so called pseudo-experiment data (or pseudo-data). For each scan point, cross section value taken from the base template is varied according to the expected statistical fluctuations (from Poisson distribution), taking selection efficiency and background contribution into account. Example of the generated pseudo-data set is shown in Fig. 4.

3.2 Minimisation method

Parameter fit procedure is then applied to the generated pseudo-data set. For each considered cross section template the χ^2 value is calculated from the formula

$$\chi^2(\vec{p},\alpha) = \sum_i \left(\frac{m_i - \alpha\cdot\mu_i(\vec{p})}{\sigma_i}\right)^2 + \left(\frac{\alpha-1}{\Delta}\right)^2 + \sum_j \left(\frac{p_j-\tilde{p}_j}{\sigma_{p_j}}\right)^2 \quad (1)$$

where m_i and σ_i are the measured cross section values with their statistical uncertainties (pseudo-data set), $\mu_i(\vec{p})$ denotes the template cross section values for corresponding collision energies and given parameter set $\vec{p} = (m_t, \Gamma_t, \alpha_s, y_t^2, f_{bg})$, and α is the template normalisation factor. The second term in the

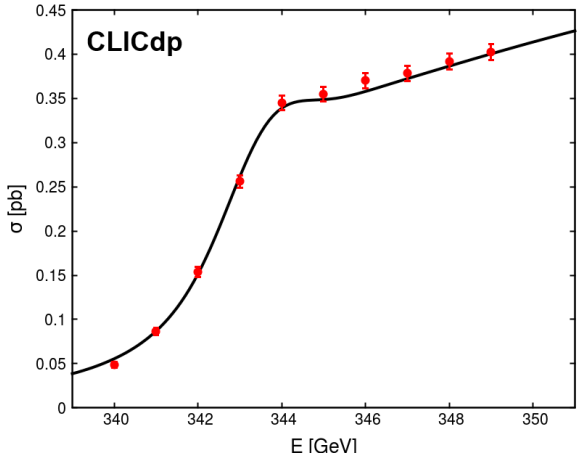

Figure 4: Reference scenario for the top-quark threshold scan. The error bars on the simulated data points show the expected statistical uncertainties of the cross section measurements assuming integrated luminosity of 10 fb^{-1} per measurement.

χ^2 formula corresponds to the normalisation constraint, where different values of the relative normalisation uncertainty Δ are considered. The normalisation factor α can be evaluated analytically separately for each template by solving the minimisation condition $\frac{\partial \chi^2}{\partial \alpha} = 0$. The third term represents possible constraints on the model parameters p_j resulting from the earlier, independent measurements with uncertainty σ_{p_j}. In this study, external constraints are considered for α_s, y_t and f_{bg}.

The values of the top-quark mass and other model parameters can then be extracted from the fit of the polynomial χ^2 dependence on the components of $\vec{p}$

$$\chi^2_\alpha(\vec{p}) = \sum_{i=0}^{N} \sum_{j=0}^{N} A_{i,j}\, p_i p_j \tag{2}$$

where χ^2_α is the χ^2 value minimised w.r.t. normalisation factor α, N is the number of considered model parameters and i, j are parameter indexes ($i, j = 1 \ldots N$). $A_{i,j}$ is the symmetric matrix of coefficients of N-dimensional parabola. To simplify the formula, $p_0 \equiv 1$ was defined (the linear part is thus given by $2A_{0,j}p_j$ and the constant part is $A_{0,0}$). The values of parameters $A_{0,0}, \ldots, A_{n,n}$ are found by solving a set of linear equations, where χ^2_α values calculated for different parameter sets $\vec{p}$ are used as input. The fitted values of $A_{0,0}, \ldots, A_{n,n}$ are then used to extract the parameter values minimising the $\chi^2_\alpha(\vec{p})$, which constitute the fit result. Statistical uncertainties of the fitted parameter values, $\vec{\sigma} = (\sigma_{m_t}, \sigma_{\Gamma_t}, \sigma_{\alpha_s}, \sigma_{y_t^2}, \sigma_{f_{bg}})$, and their correlation coefficients, $r_{i,j}$, are extracted from the fit covariance matrix.

The fitting procedure was applied to a large sample of pseudo-data sets generated for the reference scan scenario (see Fig. 4) and the nominal parameter values (see Tab. 1), taking top-quark mass and width as the only free parameters in the fit. Distribution of the fit results presented in Fig. 5 is well described by the 2-D Gaussian profile; results of the profile fit to the data are indicated by the one, two and five sigma contours indicated in the plot. For the considered 2-D fit configuration (top-quark mass vs top-quark width), fits to the marginalized parameter distributions result in σ_{m_t}=19.4 MeV and σ_{Γ_t}=49.3 MeV. These uncertainties are in a good agreement with results of the previous study [4], see Fig. 3 (right). The uncertainties estimated from parameter distributions are also in very good agreement with those extracted from the covariance matrix of the fit.

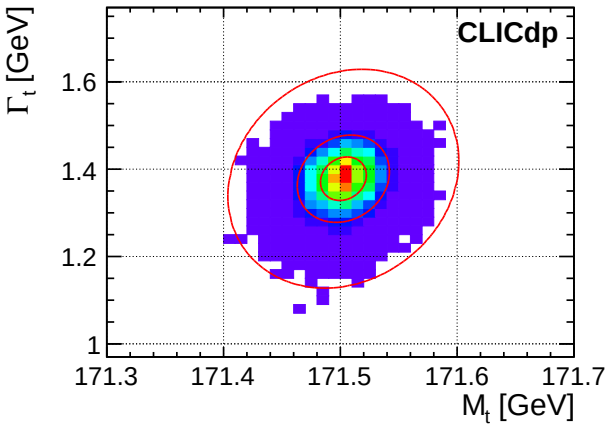

Figure 5: Results of the two-parameter fits to the top threshold scan, for sets of pseudo-data generated for nominal parameter values, $\tilde{m}_t = 171.5$ GeV and $\tilde{\Gamma}_t = 1.37$ GeV. One, two and five sigma contours represent the 2-D Gaussian distribution fitted to the presented results.

4 Baseline threshold scan results

4.1 Comparison of fit configurations

As mentioned above, study [4] considered two-parameter fits to the threshold scan data only. This is also the case for earlier studies [18, 19], while simultaneous fit of four model parameters was previously considered in [20]. Presented approach, thanks to its simple, semi-analytical form, allows to perform fits with even more free model parameters. Moreover, it is possible to add additional constraints on the selected parameters to make the fit reflect the expected experimental situation better.

Presented in Fig. 6 (left) is the expected statistical precision of the top-quark mass as the function of the assumed normalisation uncertainty, Δ, for five selected configurations of the threshold scan data fit. Precision of the one-parameter (1D) mass fit (m_t) is compared with the two-dimensional (2D) fit of mass and width ($m_t + \Gamma_t$) and different three-dimensional (3D) fit configurations. The normalisation uncertainty covers all systematics related to the overall normalisation of the data (coming from luminosity measurement, modelling of the event selection efficiency, theoretical predictions). No other constraints are imposed on the model parameters considered in these fits.

Expected top-quark mass uncertainty from the 2D fit to the threshold scan data is very close to the results of the 1D fit and sizeable differences are only observed, if normalisation is not well constrained, $\Delta > 0.01$. However, significant changes are observed when adding more parameters to the fit. While the statistical uncertainty on the top-quark mass around 20 MeV can be achieved using 1D or 2D fit procedure (i.e. mass only or mass and width fit), the uncertainty increases by over 10 MeV when adding top Yukawa coupling ($m_t + \Gamma_t + y_t$) or background level variation ($m_t + \Gamma_t + B$) to the fit. Largest deterioration of the measurement precision is observed when the strong coupling constant is considered as the free model parameter ($m_t + \Gamma_t + \alpha_s$) with uncertainty increasing by over a factor of two. This is also the fit configuration which is most sensitive to the overall normalisation of the data. To allow most precise top-quark mass determination, the normalisation has to be known on sub-percent level.

For results shown in Fig. 6 (left), no constraints were imposed on the model parameters considered in the fit. This is clearly not the proper approach for parameters describing systematic variations, which should not be considered as "free". Background contribution can be precisely estimated from theoretical predictions and Monte Carlo simulation results, the strong coupling constant is known at percent level from many experiments and Lattice QCD calculations [21]. Also the top Yukawa coupling can be constrained from independent studies at CLIC [22] or by other experiments [23]. Constraining the fit al-

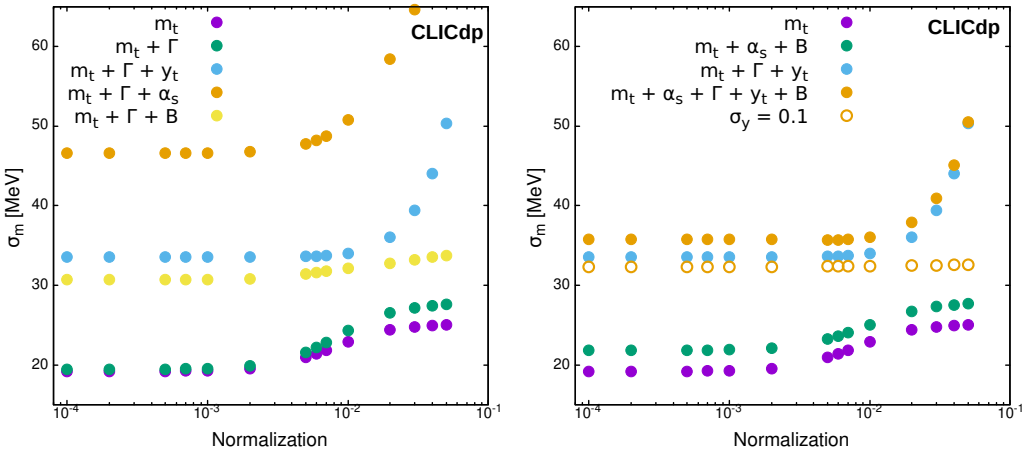

Figure 6: Statistical uncertainty on the top-quark mass as a function of the assumed overall normalisation uncertainty for different fit configurations. Left: without any additional parameter constraints. Right: for "SM constrained" mass fit (m_t) and the fit of mass, width and Yukawa coupling ($m_t + \Gamma_t + y_t$), without and with systematic parameters and their constraints included in the fit; results of the fit with additional constraint on the Yukawa coupling are also indicated, see text for details.

gorithm by assuming parameter values are known with some uncertainty from independent measurement makes the analysis closer to the situation expected in an actual experiment.

Impact of the parameter constrains on the uncertainty of the extracted top-quark mass is demonstrated in Fig. 6 (right) for two fit configurations. One-parameter fit of the top-quark mass can be considered as a model for "SM constrained" data analysis, when top-quark width and Yukawa coupling are taken from SM predictions. When two systematic parameters are added to the fit, the strong coupling constant, α_s, and the background level, f_{bg}, taking into account the corresponding constraints of $\sigma_{\alpha_s} = 0.001$ and $\sigma_{f_{bg}} = 2\%$, uncertainty of the mass fit is increased by about 2.5 MeV independent on the assumed normalisation uncertainty. Similar effect is observed for the three-dimensional fit of mass, width and Yukawa coupling ($m_t + \Gamma_t + y_t$), when no dependence between these parameters is assumed (allowing for possible BSM contribution). After adding the two systematic parameters to the fit, the uncertainty increases by about 2 MeV, except for the region of very large normalisation uncertainties, $\Delta > 0.01$ where the impact is smaller. Also shown in Fig. 6 (right) is the influence of the possible additional constraint imposed on the top Yukawa coupling, assuming $\sigma_{y_t} = 0.1$. Independent measurement of the top Yukawa coupling significantly improves the precision of the top-quark mass determination and the effect is largest for large normalisation uncertainties. In fact, with additional constraint imposed on the Yukawa coupling the expected precision of the mass determination improves to around 32 MeV and is almost independent on the assumed normalisation uncertainty. This can be attributed to the significant correlations between the parameters describing the Yukawa coupling, background level and the strong coupling constant.

4.2 Impact of constraints

As demonstrated above, constraints on model parameter resulting from measurements preceding the top threshold scan at CLIC can significantly reduce statistical uncertainties of the fit. In this section, impact of these constraints is studied in a more quantitative way. The problem can also be reversed: how precisely should other model parameters be measured in order to allow for the best possible top-quark mass determination in the threshold scan. Considered is the most general fit configuration with all model parameters included in the five-dimensional (5D) fit: top-quark mass, m_t, width, Γ_t, and the Yukawa coupling, y_t, as well ass the strong coupling constant, α_s and the background level scaling factor, f_{bg} (see

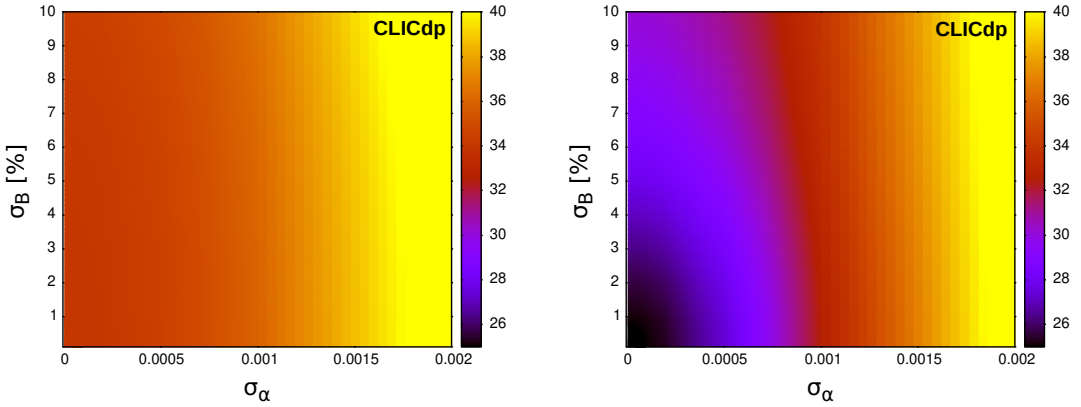

Figure 7: Expected uncertainty on the top-quark mass as a function of the uncertainty of the strong coupling constant and the background level uncertainty. Results from the fit of all model parameters (5D) are presented with no constraint on the top Yukawa coupling (left) and for the assumed Yukawa uncertainty of $\sigma_{y_t} = 0.1$ (right). Normalisation uncertainty, $\Delta = 1\%$, is assumed. Colour maps are obtained using a linear interpolation algorithm.

Tab. 1). Note that the data normalisation factor, α, the sixth model parameter, is not included in the fit procedure but is evaluated analytically for each cross section template, as described in Sec. 3.2.

Shown in Fig. 7 is the expected top-quark mass uncertainty from the 5D fit to the threshold scan data plotted as a function of the assumed strong coupling constant and background contribution uncertainties. Relative uncertainty of 1% is assumed for the overall data normalisation. Two fit scenarios are considered: with the top Yukawa coupling considered an unconstrained model parameter (left plot) and with assumed Yukawa uncertainty from earlier measurements of $\sigma_{y_t} = 0.1$ (right). If no constraint can be set on the value of the Yukawa coupling, uncertainty of the extracted top-quark mass depends mainly on the assumed uncertainty on α_s. Even if the strong coupling constant is known with very high precision, uncertainty on the mass cannot be reduced below about 34 MeV (see also 3D fit results shown in Fig. 6). The estimated top-quark mass uncertainty decreases significantly, if external constraint on the Yukawa coupling, with $\sigma_{y_t} = 0.1$, is imposed, as shown in Fig. 7 (right). However, to be able to extract top-quark mass with precision of the order of 25 MeV, strong coupling constant would need to be known with precision higher than 0.0003 and the background contribution to at least 2%. With the current uncertainty of the world average, $\sigma_{\alpha_s} = 0.001$ [21], mass uncertainty cannot be reduced below about 32 MeV. Unfortunately, uncertainty on the strong coupling constant is not likely to be significantly reduced in the near future [24].

Impact of the assumed Yukawa coupling constraint on the expected fit precision is also shown in Fig. 8. Uncertainty on the top-quark mass is presented as a function of the assumed Yukawa coupling and the strong coupling constant uncertainties (left plot), and as a function of the Yukawa coupling and the background contribution uncertainties (right plot). Presented results indicate that, although the extraction of top-quark mass does profit from additional Yukawa coupling constraint, possible improvement of the coupling determination precision beyond the assumed uncertainty of $\sigma_{y_t} = 0.1$, will hardly improve the mass determination precision. Therefore this value of uncertainty is used for the following analysis, although higher precision is expected considering combined analysis of the Higgs boson measurements at the HL-LHC [23].

As the top-quark pair-production cross section depends on the top Yukawa coupling, the threshold scan data can also be used to constrain its value. The statistical precision of the Yukawa coupling determination from the 5D fit was investigated as a function of the assumed background and strong coupling uncertainties. Results presented in Fig. 9 indicate that contribution from the Yukawa coupling can be

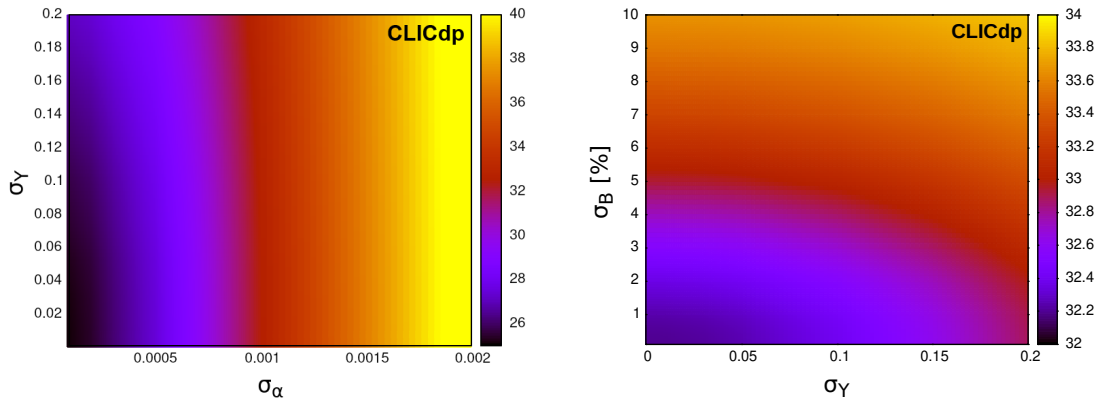

Figure 8: Expected uncertainty on the top-quark mass from the fit involving all considered model parameters (5D). Left: as a function of the strong coupling constant and Yukawa coupling uncertainties, assuming background uncertainty of 2% and normalisation uncertainty, $\Delta = 1\%$. Right: as a function of the background and Yukawa coupling uncertainties assuming strong coupling uncertainty of 0.001 and normalisation uncertainty, $\Delta = 1\%$.

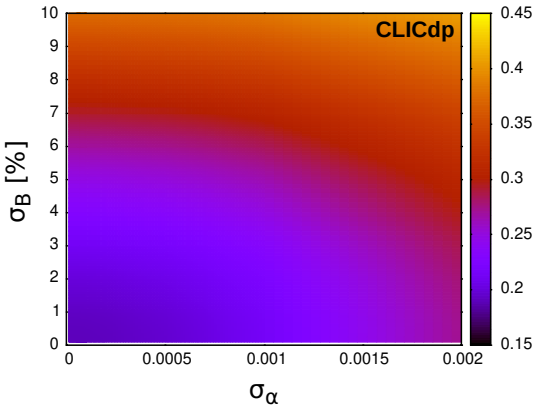

Figure 9: Expected statistical uncertainty on the top Yukawa coupling from the fit involving all considered model parameters (5D), as a function of the strong coupling constant and background contribution uncertainties. Normalisation uncertainty, $\Delta = 1\%$, is assumed.

observed in the threshold scan data with 5σ significance (i.e. with statistical precision of about 0.2) assuming the normalisation is known at percent level, the strong coupling is known better than 0.001 and the background uncertainty is below 3%.

4.3 Systematic effects

Results presented above demonstrate that systematic uncertainties are likely to limit the ultimate precision of the top-quark mass determination from the threshold scan. Various sources of uncertainties have been investigated in [4] and the combined systematic uncertainty of the top-quark mass is expected to be in range of 30 MeV to 50 MeV. In particular, the parametric uncertainty originating from the strong coupling constant was estimated to be 30 MeV (for the reduced charge luminosity spectrum considered here), also assuming an uncertainty of 0.001 in α_s. Systematic mass uncertainty resulting from the background level estimates is much smaller: for the 5% shift of the estimated background contribution 18 MeV vari-

ation is expected in the extracted top-quark mass [18], corresponding to about 7 MeV variation for the background level uncertainty of 2% assumed here.

The procedure described in this work, including parameters describing systematic effects and the corresponding constraints directly in the fit to the threshold scan data, allows for proper treatment of all uncertainties, including their correlations, resulting in a significant reduction of the total mass uncertainty. When systematic variations of the strong coupling constant and the background level are not considered, the expected statistical uncertainty of the top quark mass from the 3D fit is 34 MeV (22 MeV) without (with) additional constraint on the Yukawa coupling. With parametric uncertainties from α_s and f_{bg} variations of 30 MeV and 7 MeV, respectively, this would correspond to the total top-quark mass uncertainty of 46 MeV (38 MeV). With the proposed approach, where the threshold scan data can be also used to reduce the influence of the parameter variations, the final uncertainties (including the considered systematic effects) are 36 MeV (32 MeV), see Fig. 6. This corresponds to the reduction of the total uncertainty by 15 to 20%.

In the study [4] the dominant systematic uncertainty in the top-quark mass measurement from the threshold scan was attributed to the missing higher orders in theory calculations. This uncertainty was estimated with the variation of the QCD renormalisation scale parameter, μ, used as an input to `QQbar_threshold` calculations (see Tab. 1) and was found to be around 40 MeV. Unfortunately, this type of uncertainty cannot be included in the presented analysis framework. The main reason is that constraints on the renormalisation scale are not well defined and it is not possible to properly describe its variations in terms of the probability density function. Also, default value of the renormalisation scale used in `QQbar_threshold` calculations corresponds to the maximum value of the top-pair production cross section at the threshold [10] and the linear approximation used in the proposed fit procedure, resulting in parabolic dependence of the χ^2_α value on the model parameters (see Eq. (2)) is no longer valid. Therefore, this source of uncertainty is neglected in the presented study. One can also expect that the theoretical calculations will still improve before the threshold scan is eventually performed.

Top-quark mass parameter of the `QQbar_threshold` program is defined in the 'potential-subtracted' (PS) mass scheme [25]. While conversion of the PS mass to the $\overline{\text{MS}}$ mass scheme is a subject to additional theoretical uncertainties, this is also beyond the scope of this paper.

4.4 Initial mass uncertainty

The nominal procedure of pseudo-experiment generation starts from selecting the 'true' model parameters, including the true value of top-quark mass. Nominal mass value, as listed in Tab. 1, was used for all the results presented so far. However, the mass value will only be known with limited precision before the actual experiment takes place, so the position of the scan energy points w.r.t. the true mass will not be known. To verify how this affects the expected scan results, fit procedure was repeated multiple times assuming top-quark mass is known with given uncertainty. For each set of pseudo-experimental data true mass value was drawn from normal distribution with given spread, σ_m. By creating large sets of pseudo-data with different initial mass spread, it is possible to study how the initial mass uncertainty influences results of our algorithm.

Presented in Fig. 10 are distributions of the top-quark mass uncertainty from the 5D fit assuming different initial top-quark mass variations: $\sigma_m = 0$ MeV (fixed 'true' mass), 200 MeV (corresponding to the projected HL-LHC experimental uncertainty [26]) and 1000 MeV. The three distributions overlap almost perfectly showing that the initial uncertainty in the top-quark mass has hardly any influence on the precision of the top mass determination. This lack of sensitivity seems counter intuitive, but this is the feature of the reference scan scenario, with equidistant energy points covering wide energy range. The loss in precision is negligible even in the case of significant change in the initial top-quark mass value.

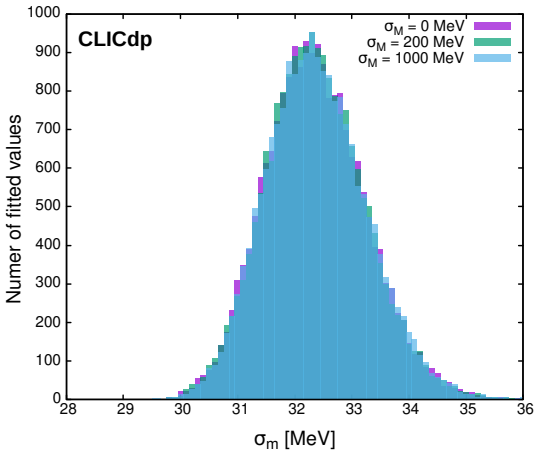

Figure 10: Histograms of fitted uncertainties for the top-quark mass, assuming drawing true mass value from Gaussian distribution of different width.

5 Scan optimisation

5.1 Multi-objective optimisation

When looking for the best scenario of the top-quark threshold scan at CLIC (or at any other future e^+e^- collider) one needs to consider different aspects of the measurement. The top quark mass is not the only parameter that needs to be extracted (with the best possible statistical uncertainty). There are other model parameters, measurement of which needs to be optimised at the same time. Multi-objective optimisation problems are likely to be complex and must be approached differently, depending on the specific case. When looking for the best optimisation approach it is necessary to take into account, for example, how easy it is to find solution to the considered problem and how many solutions are expected. It could be that there are so many possible solutions that all of them cannot be analyzed.

The easiest case is when one can propose a set of equations describing the problem, defining the variables to be optimised. These equations can be then solved analytical or numerically, to find the optimum. Yet, it is rarely the case when the problem can be reduced to such a set of equations.

In most real-world problems, heuristic procedures are being used to find optimal solutions. They include Genetic algorithms, that are inspired by biological evolution processes, such as reproduction, mutation, recombination, and selection [27]. In a Genetic algorithm, a set of proposed solutions to an optimisation problem, called *Individuals*, is evolved towards better solutions. Each Individual has a defined set of properties, called *genotype*, which can be mutated and altered, and set of measurable traits, called *phenotype*, that are determined by the genotype. Phenotype consists of traits that are used to evaluate their performance and choose the best Individuals to the next generation. During consecutive iterations of the algorithm population evolves towards better solutions. Ultimately, after a finite number of iterations, population should converge to the optimal solution.

5.2 Non dominated sorting genetic algorithm II

From many available Genetic algorithms, Non dominated sorting genetic algorithm II, proposed by Kalyanmoy Deb in 2002 [28], was chosen for this study, for its high efficiency and elasticity. Each iteration of the algorithm is divided into three steps:

- Creating Children and adding them into population
- Non dominated sorting of the population (with Jensen algorithm [29])

- Choosing the best Individuals for the next generation

Each one of those steps is highly customizable, so it is possible to adjust the implementation in order to achieve the best results. Thanks to use of efficient non dominated sorting algorithm it was possible to lower time complexity from original $O(MN^2)$ [28] to $O(MNlog^{M-1}N)$ [29], where M is number of objectives and N is the size of the population.

5.2.1 Creating Individuals and First Generation

The first step was to translate our measurement procedure into Genetic algorithm language. One measurement scenario was assumed as an Individual, which genotype is represented by a scan sequence, set of centre-of-mass energy points (scan points make a multiset, as they can repeat, but their order is irrelevant). In this way each scan point can be considered a chromosome. Constant total integrated luminosity of $100\,\mathrm{fb}^{-1}$ was assumed and its equal sharing among all scan points. This might seem restrictive, but scan points with higher luminosity are actually allowed by allowing energy points to repeat in the scan sequence. This way it is also possible to optimise luminosity distribution. The measurement procedure described in previous chapters translates scan sequence (genotype) into measured top quark parameters with their uncertainties (phenotype). Yet, this process is non-deterministic, as statistical fluctuations were drawn from Poisson distribution separately for each generated pseudo-data set. To take statistical fluctuations into account pseudo-experiment procedure is always repeated three times and the worst result for each objective is taken.[1] The First Generation is seeded by creating 2000 identical Individuals using baseline scenario. Results presented in Chapter 4 show that it provides good fit results for all parameters.

5.2.2 Pairing and breeding Individuals

There are many proposed strategies to find the best pair of parents, but they are computationally costly. In order to ensure diversity in population, each Individual has three children, one with each of three other, randomly chosen Individuals. This method was used because of computational efficiency and for maximizing diversity in population. After obtaining two parent genotypes, it is necessary to ensure they are of the same length before making a new one (a child). It was done by inserting empty chromosomes into a shorter one, to mach their sizes. While iterating over parental genotypes, parent chromosome to insert into child's genotype is chosen randomly. To allow changing genotype length, 5% chance to drop any of the chromosomes was added. To avoid systematic loss of chromosomes, additional random chromosome was added at the end of the genotype with a 10% probability. It was always required that the length of the resulting genotype is not shorter than 2, as shorter ones cannot be used for the phenotype evaluation (threshold fit procedure). When copying parent chromosome, it is also shifted by a random mutation in a given range. At the beginning of the evolution, the mutation range is $\pm 0.5\,\mathrm{GeV}$, but it shrinks geometrically in each iteration by factor of 0.9. In this way, it was possible to quickly mutate the initial baseline scenario without loosing the ability to converge around the best solution after a larger number of iterations. After creating all children in the generation their phenotypes were computed and they were inserted into the population.

5.2.3 Performance evaluation and selecting the next Generation

When considering more than one objective in the scan optimisation, one cannot simply compare (and sort) Individuals by their phenotype (parameter uncertainties from the fit). Instead, desired configuration is Pareto efficiency, which is defined as a configuration that cannot be modified so as to improve any objective without making at least one other objective worsen [30]. In order to find optimal solution

[1] The number of pseudo-experiments run for each Individual is limited by the processing time. However, already with three experiments the possible bias of the optimisation due to statistical fluctuations is basically excluded.

Individuals must be compared with each other. To find which one is better, their Pareto dominance must be checked, which is the situation when one Individual is better in at least one objective, and not worse in all other [30]. The condition for Individual x dominating Individual y, $x \succ y$, can be described by the formula:

$$x \succ y \iff \forall_i : f_i(x) \geq f_i(y) \wedge \exists_j : f_j(x) > f_j(y) \tag{3}$$

where $f_i(x)$ denotes objective i calculated for Individual x. When neither of them dominate the other, then the two Individuals are Pareto efficient. Individuals were grouped based on this criteria and such groups are called Pareto Frontiers [30]. They can by described by the formula:

$$P(Y) = \{y' \in Y : \{y'' \in Y : y'' \succ y'\} = \emptyset\} \tag{4}$$

Individuals were chosen for the next generation by sorting Pareto frontiers. It is based on criteria that a solution in $Front_{k+1}$ must be dominated by at least one solution in $Front_k$ and may or may not dominate solutions in $Front_{k+2}$ [31]. To efficiently perform those calculations Jensen algorithm was used [29]. After sorting Pareto frontiers, 2000 Individuals from frontiers with lowest ranks were selected for the next generation.

5.3 Results

5.3.1 Single objective

The performance of the optimisation procedure based on the Genetic algorithm was first studied for the optimised measurement of one model parameter only: top-quark mass, top-quark width or top Yukawa coupling. The objective is to minimize the statistical uncertainty resulting from the fit of the given parameter in a most general (5D) fit procedure, with all model parameters taken into account. Population size is set to 2000 and number of generations to 30. All results presented in this section were calculated assuming normalisation uncertainty of $\Delta = 0.1\%$, strong coupling constant uncertainty of $\sigma_{\alpha_s} = 0.001$ and background level uncertainty of $\sigma_{f_{bg}} = 2\%$. When measurement of the top Yukawa coupling was not included in the optimisation objectives, uncertainty of $\sigma_{y_t} = 0.1$ was assumed for constraint coming from independent coupling measurement.

Results of the optimisation procedure for the three considered model parameters are summarised in Fig. 11. When the scan procedure is optimised for the top-quark mass determination, the measurement is focused in three energy regions, with most of the luminosity taken in the middle of the threshold (around 343 GeV), where the cross section slope is highest, and at the plateau just above the threshold (around 345 GeV), see top left plot in Fig. 11. With this choice of measurement points, it is possible to reduce the expected uncertainty of the top-quark mass by about 30%, from 32 MeV expected for the ten-point baseline scan scenario to 22 MeV for the optimised ones.

However, the scenario optimised for mass measurement is clearly not the best one when the top-quark width measurement is considered. In this case, much larger fraction of the luminosity should be devoted to the cross section measurement just below the threshold (around 341 GeV), see top right plot in Fig. 11. With the width-optimised scan scenario, the statistical uncertainty on the top-quark width is reduced by about 40%, from 58 MeV for the baseline scenario to around 35 MeV for the optimal ones.

Smallest improvement due to scan optimisation can be obtained for the top Yukawa coupling measurement. As shown in Fig. 11 (bottom plot), in order to constrain the Yukawa coupling better, significant fraction of the luminosity has to be taken above the threshold, at around 350 GeV. This allows for about 20% improvement in the precision of the top Yukawa coupling determination, from about 0.18 to 0.14.

Looking at the measurement point distributions in Fig. 11 one can clearly see that four energy regions are relevant in the scan optimisation: energies just below the threshold (around 340-341 GeV), in the middle of the threshold (around 343 GeV), on the plateau just above the threshold (around 345 GeV) and further above the threshold (around 349-350 GeV). Different regions are sensitive to different model

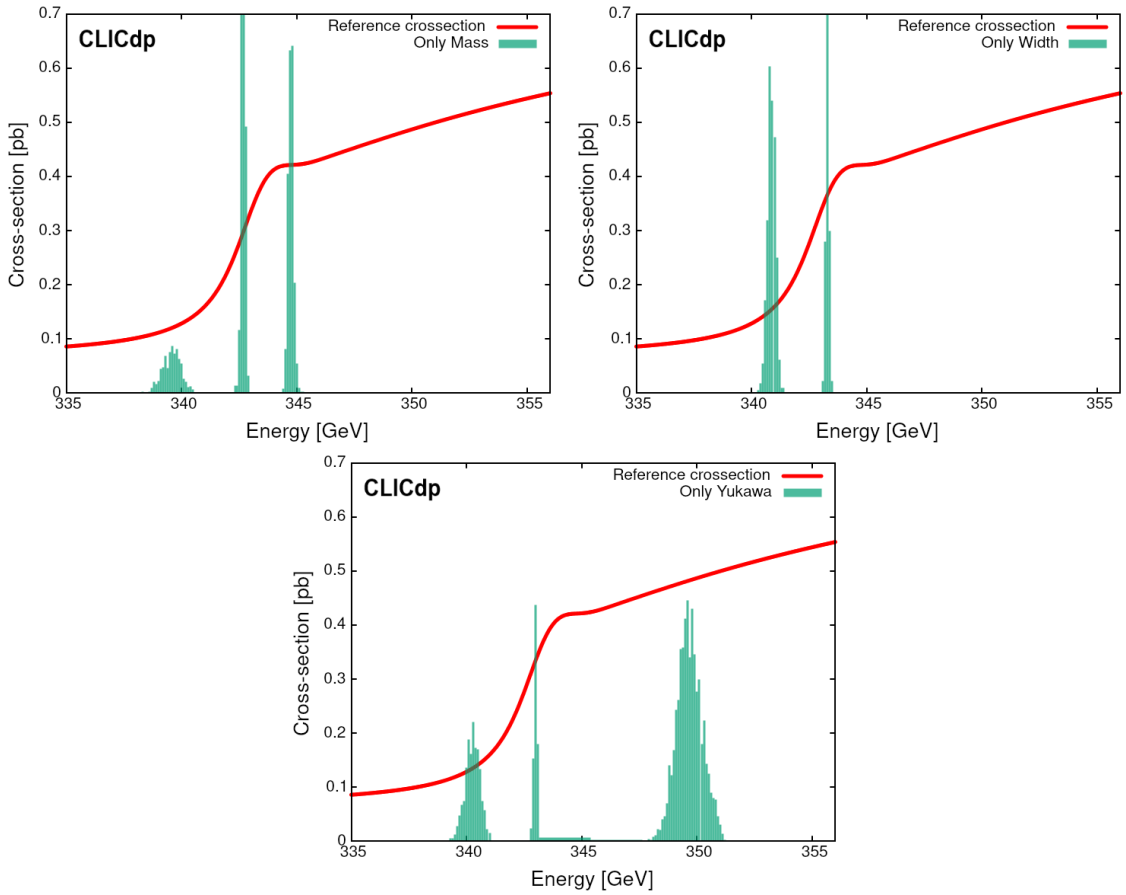

Figure 11: Distribution of the measurement points from last generation (arbitrary scale) compared with the reference cross section template, for three single parameter optimisation scenarios: top-quak mass (top left), top-quark width (top right) and top Yukawa coupling (bottom plot) measurement optimisation.

parameters: the regions in the middle and just above the threshold are most relevant for the mass measurements, measurement below the threshold is crucial for the width measurement, whereas the Yukawa coupling determination depends on the amount of luminosity which can be devoted to running few GeV above the threshold. This comparison shows that the same choice of energy points can be optimal (or close to optimal) for all considered parameters. However, sharing of the luminosity between four energy regions depends on the optimisation goal.

5.3.2 Multiple objectives

When considering multiple objectives, it was decided to focus on pairs of top-quark parameters, in order to study how they influence each other in the optimisation procedure. Shown in Fig. 12 are the results of mass and width measurement optimisation. For both parameters, improvement of about 20-25% can be achieved: mass uncertainty is reduced by about 6 MeV, from 32 MeV to 26 MeV, while the width uncertainty is reduced by about 14 MeV, from 58 MeV to 44 MeV. The improvement is smaller, when compared to single objective optimisation, by 10-15% (about 4 MeV for mass and 9 MeV for width uncertainty). As expected, the optimised measurement point distribution combines the scenarios obtained for one parameter mass and width optimisations (see Fig. 11). Most of the scenarios from the last generation, more than 99%, include 5 energy points, showing good convergence of the optimisation.

When optimising the scan procedure for simultaneous top-quark mass and top Yukawa coupling meas-

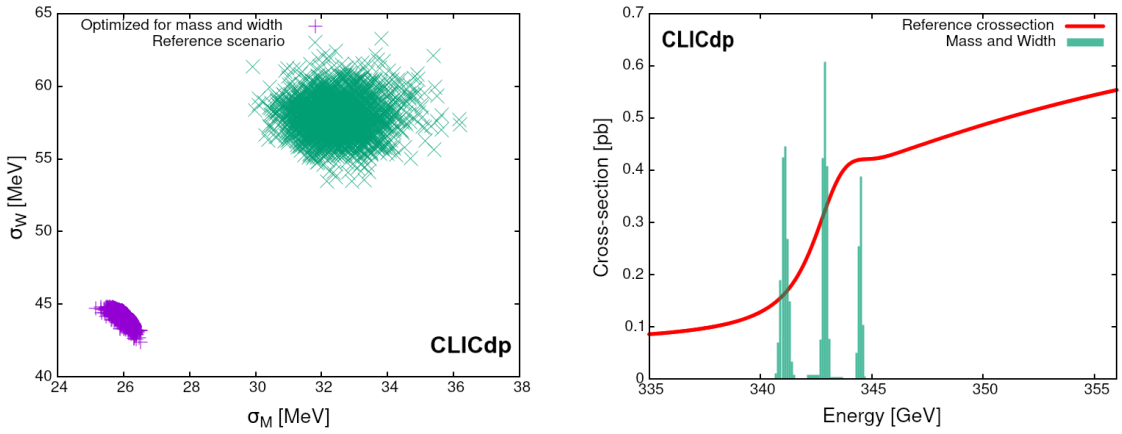

Figure 12: Left: mass and width uncertainty distribution in the first (green) and the last (blue) generation for scan optimised for both mass and width determination precision. Right: distribution of the measurement points from the last generation (arbitrary scale) compared with the reference cross section template.

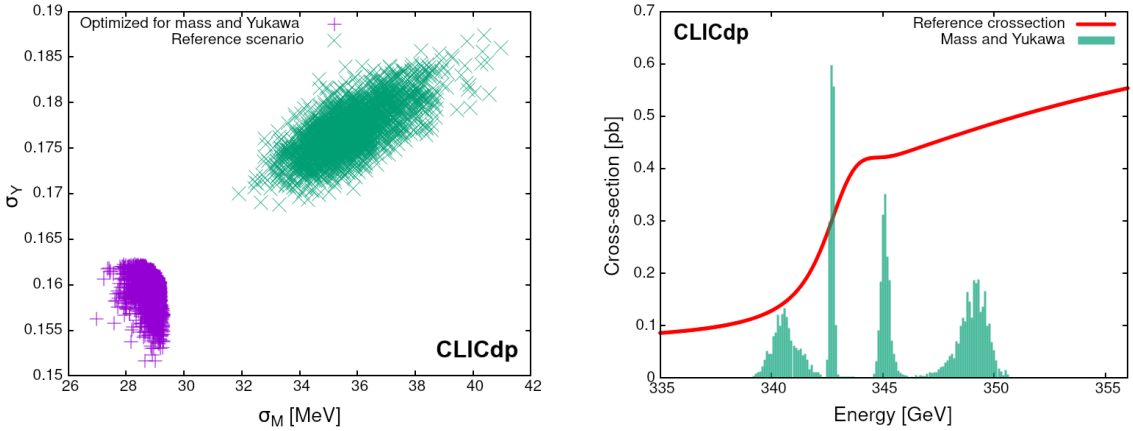

Figure 13: As in Fig. 12 but for scan optimised for mass and Yukawa coupling determination precision.

urement, see Fig. 13, results are again similar to those obtained for one objective optimisation. Note that possible constraint on the Yukawa coupling is not taken into account for this optimisation. Improvement of about 22% can be expected for the mass measurement, from 36 MeV to 28 MeV, but only about 10% improvement in the Yukawa coupling uncertainty. The measurement point distribution for this optimisation scenario is very similar to the one obtained for Yukawa only optimisation (see bottom plot in Fig. 11), but with additional measurements just above the threshold (at about 345 GeV) required for precise mass determination. More scan points are also required for the optimal measurement in this case: 97% of the last generation scenarios consist of 9 or 10 measurement points.

For detailed comparison of the optimised scenarios with the baseline threshold scan configuration, one scenario was selected from the last generation for each of the aforementioned multi objective optimisations. Two selected scenarios are presented in Fig. 14: five-point scenario optimised for mass and width measurement and ten-point one, optimised for mass and Yukawa coupling. In both scenarios points group in pairs, in places where more luminosity should be collected (at the threshold and, in case of mass and Yukawa optimisation, just above the threshold). These "best scenarios" were compared with the reference scenario based on results coming from 20 000 pseudo-experiments. As before, normalisation uncertainty is $\Delta = 0.1\%$, strong coupling uncertainty is $\sigma_{\alpha_s} = 0.001$, background level uncertainty is $\sigma_{f_{bg}} = 2\%$ and, for mass and width optimisation, Yukawa uncertainty of $\sigma_{y_t} = 0.1$ is assumed. To

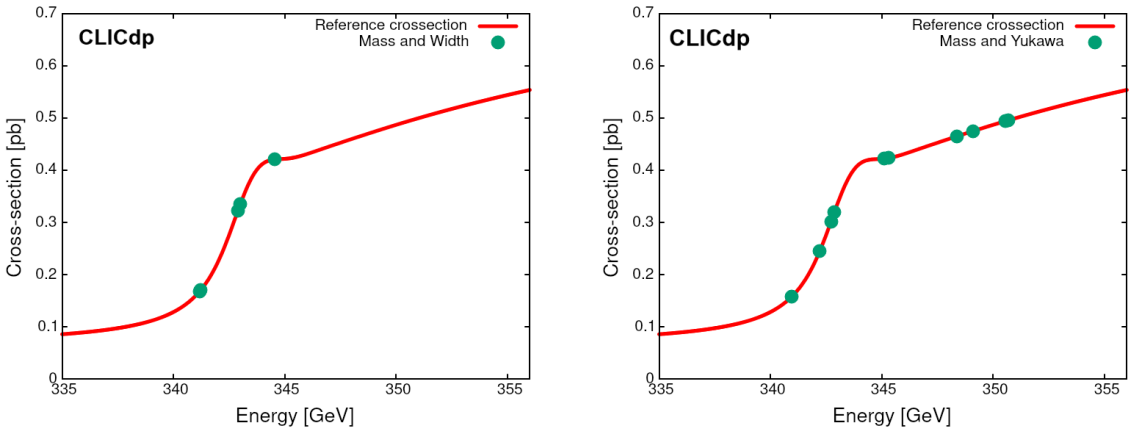

Figure 14: Scan energy points for the "best scenarios" taken from the last generation compared with the reference cross section template: (left) 5 point scenario optimised for mass and width determination precision (two points below, two in the middle and one above the threshold) and (right) 10 point scenario optimised for mass and Yukawa coupling determination precision.

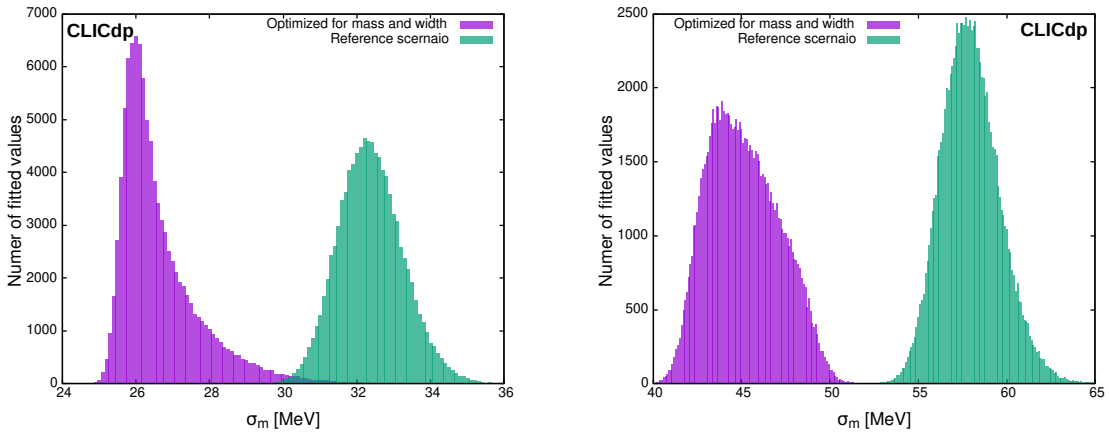

Figure 15: Uncertainty distribution for mass (left) and width (right) measurement, for five-point scan scenario optimised for mass and width measurement (see Fig. 14), compared with the distributions for the reference scenario.

make comparison even more realistic, 'true' top quark mass is varied in the pseudo-data generation procedure to model its initial uncertainty of 200 MeV, corresponding to the projected future experimental uncertainty of top-quark mass measurement at HL-LHC [26].

Results of the comparison for the five-point scenario are presented in Fig. 15. Shown are the distributions of uncertainties on the top-quark mass and width. Results based on large sample of pseudo-experiments confirm estimates obtained from the optimisation procedure (where each scenario was evaluated based on three pseudo-experiments only). For the optimised scenario most probable value of expected mass uncertainty is around 26 MeV, while for width it is around 44 MeV.

When searching for the "best" threshold scan scenario, looking just at the most probable or expected uncertainty values is not enough. The shape and width of the uncertainty distributions are also very important, showing the sensitivity of the scenario to statistical fluctuations in the experimental data and to the uncertainty of the initial top-quark mass. Distributions presented in Fig. 15 confirm that the optimised scenario will always give better results that the reference one, although the mass determination precision can deteriorate due to statistical fluctuations up to about 30 MeV. For both mass and width measurement, widths of the uncertainty distributions for the optimised scenario and for the reference one are similar.

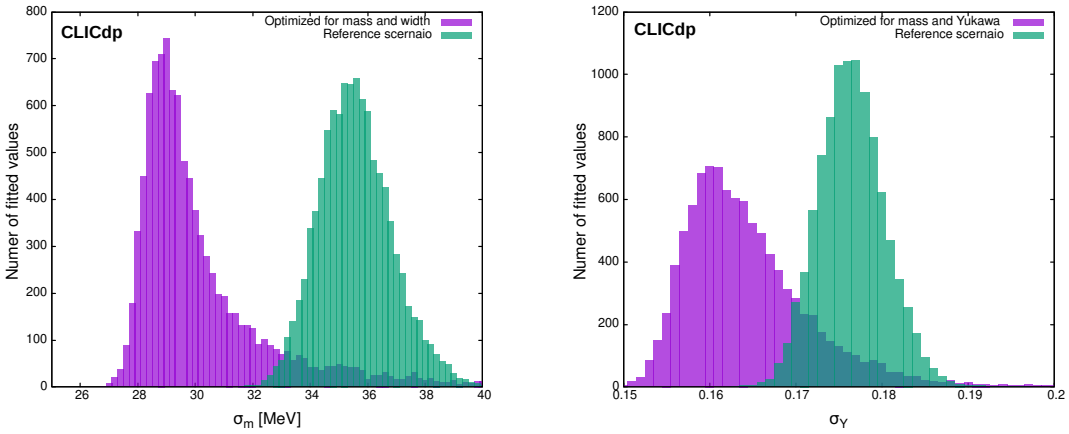

Figure 16: Uncertainty distribution for mass (left) and Yukawa coupling (right) measurement, for 8 point scan scenario optimised for mass and Yukawa coupling measurement (see Fig. 14), compared with the distributions for the reference scenario.

For scenario optimised for mass and Yukawa coupling measurement, results obtained with large sample of pseudo-experiments shown in Fig. 16 are again in good agreement with optimisation results (see Fig. 13). Uncertainty distribution for the mass measurement is similar to the one obtained for mass and width optimised scenario (Fig. 15), but slightly wider. Larger tail towards high uncertainty values results in a finite probability that the mass uncertainty from the optimised scenario is similar, or even larger than the nominal uncertainty expected for the baseline scan scenario. Similar tail towards high uncertainty values is also visible for the Yukawa coupling uncertainty distribution. Still, chance of getting worse measurement than in the reference scenario is very small and probability of observing Yukawa coupling contribution to the pair-production cross section with statistical significance higher than 5σ (corresponding to the statistical uncertainty below 0.2) is still very high.

5.3.3 Influence of the luminosity spectra

All results presented so far were obtained assuming $100\,\text{fb}^{-1}$ of data collected during the top threshold scan at CLIC. This luminosity is not sufficient to reach statistical uncertainty below 20 MeV, which was considered as a goal in the previous study [4]. However, fit uncertainties can be significantly reduced, if more luminosity is collected at the threshold. Expected measurement precision is also sensitive to the assumed shape of the luminosity spectra.

Dependences of the expected mass and width uncertainties on the integrated luminosity of the threshold scan are shown in Fig. 17. CLIC estimates are compared with results of the same analysis and optimisation procedure applied when assuming ILC [32] or FCC-ee [33] luminosity spectra. Note that the choice of the optimal scenario does change with the change of luminosity spectra. For ILC spectra, about 90% of scenarios from the last generation of mass and width optimisation include 6 energy points. Six point optimised scenario was therefore selected for the comparison. Similarly, seven-point scenario was used for FCC-ee, as this was the final number of energy points in all scenarios of the last generation. Note that only the luminosity spectra was changed for this comparison; reconstruction efficiency and background level estimated from the CLIC study [18] were used for all spectra and the possible influence of the beam polarisation was not considered.

Due to additional constraints imposed on the data normalisation, background contribution, the strong coupling constant and Yukawa coupling, the expected uncertainties decrease slower than with $\sqrt{\mathscr{L}}$. In order to achieve 20 MeV mass uncertainty, about $400\,\text{fb}^{-1}$ of data is required with reference running scenario at CLIC and about $200\,\text{fb}^{-1}$ at FCC-ee. The optimised scenarios can reach this level of precision

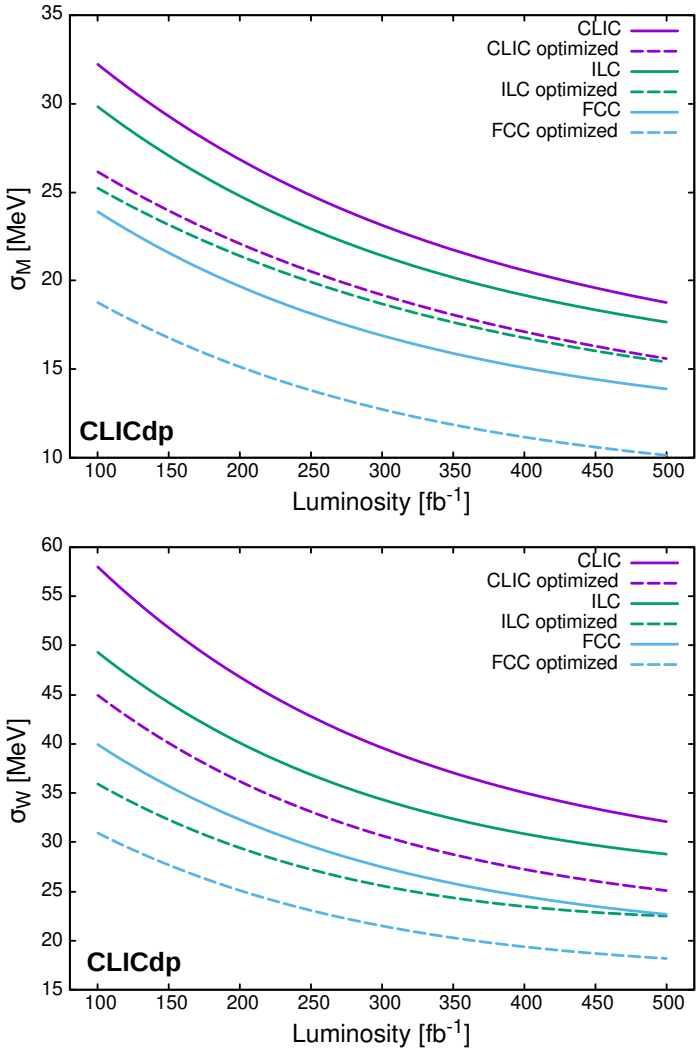

Figure 17: Expected uncertainty on the top-quark mass (top) and width (botom) from the baseline scan scenario (solid lines) and from scenarios optimised for mass and width measurement (dashed lines), as a function of the total scan luminosity. CLIC results (magenta) are compared with results of the same analysis and optimisation procedure but assuming ILC (green) or FCCee (cyan) luminosity spectra.

already with about 250 fb^{-1} at CLIC and below 100 fb^{-1} at FCC-ee. This shows clear advantage of optimised scenarios, as they can provide same precision as the reference scenario with the luminosity lower by roughly a factor of 2.

As described above, results presented in Fig. 17 were obtained for the most general 5D fit approach. When the "SM constrained" 3D fit is performed to the same scan data, with top-quark width and Yukawa coupling taken from the SM predictions, mass uncertainty from the scan scenario optimised for CLIC is reduced by about 2 MeV for the whole range of the integrated luminosity values. It is also interesting to notice that very similar mass uncertainties are obtained after the optimisation procedure for CLIC and ILC luminosity spectra. On the other hand, much higher width precision is obtained for the ILC. This is due to the fact that, compared to the five point scenario optimal for CLIC, the scenario optimised for ILC includes additional scan point in the region below the threshold (at around 341 GeV) improving the width determination, but reducing the luminosity collected at the higher energy points (more relevant for mass determination).

Presented results confirm that the optimisation procedure based on Genetic algorithm can be used to propose different running scenarios. It is possible to improve precision of top-quark mass determination by about 20%, also improving the measurement of the top-quark width or top Yukawa coupling at the same time. With optimised running scenario, the statistical uncertainties on mass and width are similar to the uncertainties expected for the reference scenario with doubled integrated luminosity (200 fb^{-1}).

6 Conclusions

Complementary fit and optimisation procedures have been developed for the top-quark threshold scan analysis at CLIC. The new fit procedure is more flexible that the one used in the previous study [4] and allows to include all relevant model parameters as well as additional constraints on model parameters, coming eg. from earlier measurement, and constraints on data normalisation. For the baseline scan scenario assumed at CLIC, with 100 fb^{-1} of integrated data luminosity, top quark mass can be measured with uncertainty of 32 MeV assuming the current uncertainty of the strong coupling constant, relative uncertainty of the Yukawa coupling of 0.1 and the background normalisation to be better than 2%. At the same time, cross section contribution from the top Yukawa coupling can be confirmed with statistical significance higher that 5σ. To improve the mass determination precision to below 25 MeV the strong coupling constant would need to be known with uncertainty below 0.0003.

Optimisation procedure based on non dominated sorting genetic algorithm II has been applied to the top-quark pair-production threshold scan. Each measurement scenario (set of energy points with total equally distributed luminosity of 100 fb^{-1}) is considered a genotype and results of the fit procedure constitute a phenotype. Implementation of the genetic evolution, starting from the baseline scenario, includes random mutations: mixing of parent genotypes, possibility to drop or gain a new (random) chromosome (scan point). Stable optimisation results are obtained for population size of 2000 and number of generation of 30. Using single and multi objective optimisation, it was shown that optimisation procedure can reduce the mass uncertainty by up to 30%. With the proposed procedure, reduction of the mass uncertainty from the top threshold scan fit should be possible, corresponding to about a factor of 2 increase in the integrated luminosity. For the optimised running scenario statistical uncertainty on the top-quark mass of 20 MeV can be reached at CLIC with 250 fb^{-1}.

Acknowledgements

The work was carried out in the framework of the CLIC detector and physics (CLICdp) collaboration. We acknowledge partial use of the earlier results from K. Debski [17]. We thank collaboration members for fruitful discussions, valuable comments and suggestions. The work was partially supported by the National Science Centre (Poland) under OPUS research projects no. 2017/25/B/ST2/00496 (2018-2021).

References

[1] M. Aicheler et al., eds.,
A Multi-TeV Linear Collider based on CLIC Technology: CLIC Conceptual Design Report,
CERN-2012-007, CERN, 2012, DOI: 10.5170/CERN-2012-007.

[2] *The Compact Linear Collider (CLIC) - Project Implementation Plan*,
4/2018 (2018), ed. by M. Aicheler et al., DOI: 10.23731/CYRM-2018-004,
arXiv: 1903.08655 [physics.acc-ph].

[3] H. Abramowicz et al., *Higgs physics at the CLIC electron–positron linear collider*,
Eur. Phys. J. C **77** (2017) 475, DOI: 10.1140/epjc/s10052-017-4968-5,
arXiv: 1608.07538 [hep-ex].

[4] H. Abramowicz et al., CLICdp,
Top-Quark Physics at the CLIC Electron-Positron Linear Collider, JHEP **11** (2019) 003,
DOI: 10.1007/JHEP11(2019)003, arXiv: 1807.02441 [hep-ex].

[5] V. S. Fadin, V. A. Khoze, *Threshold Behavior of Heavy Top Production in e^+e^- Collisions*,
JETP Lett. **46** (1987) 525.

[6] V. S. Fadin, V. A. Khoze,
Production of a pair of heavy quarks in e^+e^- annihilation in the threshold region,
Sov. J. Nucl. Phys. **48** (1988) 309.

[7] M. J. Strassler, M. E. Peskin, *The Heavy top quark threshold: QCD and the Higgs*,
Phys. Rev. D **43** (1991) 1500, DOI: 10.1103/PhysRevD.43.1500.

[8] A. H. Hoang, T. Teubner,
Top quark pair production close to threshold: Top mass, width and momentum distribution,
Phys. Rev. D **60** (1999) 114027, DOI: 10.1103/PhysRevD.60.114027,
arXiv: hep-ph/9904468.

[9] F. Simon, *A First Look at the Impact of NNNLO Theory Uncertainties on Top Mass Measurements at the ILC*, Proceedings, International Workshop on Future Linear Colliders (LCWS15): Whistler, B.C., Canada, November 02-06, 2015, arXiv:1603.04764, 2016,
arXiv: 1603.04764 [hep-ex], URL:
https://inspirehep.net/record/1427722/files/arXiv:1603.04764.pdf.

[10] F. Simon, *Scanning Strategies at the Top Threshold at ILC*,
International Workshop on Future Linear Colliders, 2019, arXiv: 1902.07246 [hep-ex].

[11] K. Nowak, A. F. Żarnecki,
Prospects for improving top-quark mass measurement precision at future e^+e^- colliders,
Proc.SPIE **10808** (2018) 1080840, DOI: 10.1117/12.2501488.

[12] K. Nowak, A. F. Żarnecki,
Extracting the top-quark mass and Yukawa coupling from the threshold scan at CLIC,
Proc. SPIE **11176** (2019) 1117648, DOI: 10.1117/12.2536861.

[13] K. Nowak, *Optimising top-quark threshold scan at CLIC using genetic algorithm*,
University of Warsaw, 2020, URL: https://cds.cern.ch/record/2728555.

[14] K. Nowak, *Optimising top-quark pair-production threshold scan at future e^+e^- colliders*,
PoS **ICHEP2020** (in print) 337.

[15] M. Beneke et al., *Near-threshold production of heavy quarks with QQbar_threshold*,
Comput. Phys. Commun. **209** (2016) 96, DOI: 10.1016/j.cpc.2016.07.026,
arXiv: 1605.03010 [hep-ph].

[16] M. Beneke et al.,
Non-resonant and electroweak NNLO correction to the e^+e^- top anti-top threshold,
JHEP **02** (2018) 125, DOI: 10.1007/JHEP02(2018)125,
arXiv: 1711.10429 [hep-ph].

[17] K. Debski, *Optymalizacja procedury wyznaczania masy kwarku top w przyszłych akceleratorach e^+e^-*, report from the advanced laboratory excersise (in Polish),
Faculty of Physics, University of Warsaw, 2018.

[18] K. Seidel et al., *Top quark mass measurements at and above threshold at CLIC*,
Eur. Phys. J. **C73** (2013) 2530, arXiv: 1303.3758 [hep-ex].

[19] T. Horiguchi et al., *Study of top quark pair production near threshold at the ILC*,
arXiv:1310.0563, 2013, arXiv: 1310.0563 [hep-ex].

[20] M. Martinez, R. Miquel,
Multiparameter fits to the t anti-t threshold observables at a future e^+e^- linear collider,
Eur. Phys. J. C **27** (2003) 49, DOI: 10.1140/epjc/s2002-01094-1,
arXiv: hep-ph/0207315.

[21] P. A. Zyla et al., Particle Data Group, *Review of Particle Physics*, PTEP **2020** (2020) 083C01,
DOI: 10.1093/ptep/ptaa104.

[22] R. Franceschini et al., *The CLIC Potential for New Physics*,
CERN Yellow Rep. Monogr. **3** (2018), ed. by J. de Blas, DOI: 10.23731/CYRM-2018-003,
arXiv: 1812.02093 [hep-ph].

[23] M. Cepeda et al., *Report from Working Group 2: Higgs Physics at the HL-LHC and HE-LHC*,
CERN Yellow Rep. Monogr. **7** (2019), ed. by A. Dainese et al. 221,
DOI: 10.23731/CYRM-2019-007.221, arXiv: 1902.00134 [hep-ph].

[24] R. K. Ellis et al.,
Physics Briefing Book: Input for the European Strategy for Particle Physics Update 2020 (2019),
arXiv: 1910.11775 [hep-ex].

[25] M. Beneke, *A Quark mass definition adequate for threshold problems*,
Phys. Lett. **B434** (1998) 115, DOI: 10.1016/S0370-2693(98)00741-2,
arXiv: hep-ph/9804241 [hep-ph].

[26] P. Azzi et al.,
Report from Working Group 1: Standard Model Physics at the HL-LHC and HE-LHC,
CERN Yellow Rep. Monogr. **7** (2019), ed. by A. Dainese et al. 1,
DOI: 10.23731/CYRM-2019-007.1, arXiv: 1902.04070 [hep-ph].

[27] M. Mitchell, *An Introduction to Genetic Algorithms*, Cambridge, MA: MIT Press., 1996,
ISBN: 9780585030944.

[28] K. Deb et al., *A Fast Elitist Non-dominated Sorting Genetic Algorithm for Multi-objective Optimization: NSGA-II*, Parallel Problem Solving from Nature PPSN VI,
ed. by M. Schoenauer et al., Springer Berlin Heidelberg, Berlin, Heidelberg, 2000, p. 849.

[29] M. T. Jensen,
Reducing the run-time complexity of multiobjective EAs: The NSGA-II and other algorithms,
IEEE Transactions on Evolutionary Computation **7** (2003) 503.

[30] V. Pareto, *Cours d'Economie Politique*, Pouge, 1896.

[31] H. Fang et al., *An Efficient Non-dominated Sorting Method for Evolutionary Algorithms*,
Evolutionary Computation **16** (2008), PMID: 18811246 355,
DOI: 10.1162/evco.2008.16.3.355,
eprint: https://doi.org/10.1162/evco.2008.16.3.355,
URL: https://doi.org/10.1162/evco.2008.16.3.355.

[32] P. Bambade et al., *The International Linear Collider: A Global Project* (2019),
arXiv: 1903.01629 [hep-ex].

[33] A. Abada et al., FCC, *FCC Physics Opportunities*, Eur. Phys. J. **C79** (2019) 474,
DOI: 10.1140/epjc/s10052-019-6904-3.